

# Elevated ATF4 Function in Fibroblasts and Liver of Slow-Aging Mutant Mice

Weiquan Li<sup>1</sup> and Richard A. Miller<sup>1,2</sup>

<sup>1</sup>Department of Pathology and  
<sup>2</sup>Geriatrics Center, University of Michigan, Ann Arbor

Address correspondence to Richard A. Miller, MD, PhD, Department of Pathology and Geriatrics Center, University of Michigan, BSRB 3001, 109 Zina Pitcher Place, Ann Arbor, MI 48109-2200. Email: [millerr@umich.edu](mailto:millerr@umich.edu)

Work in yeast has shown that longevity extension induced by nutrient deprivation, altered ribosomal function, or diminished target of rapamycin action requires the activity of GCN4. We hypothesized that increased activity of ATF4, the mammalian equivalent of yeast GCN4, might be characteristic of mutations that extend mouse life span. Fibroblasts from the skin of two such mutants (Snell dwarf and PAPP-A knockout) were found to have higher levels of ATF4 protein and expression of several ATF4 target genes in responses to amino acid withdrawal, cadmium, hydrogen peroxide, and tunicamycin. ATF4 pathways were also elevated in liver of both kinds of long-lived mutant mice. Thus, a connection between ATF4 pathways and longevity may have deep evolutionary roots, and further studies of ATF4 mechanisms may provide insights into the links between cellular stress resistance, protein translation control, and aging.

**Key Words:** ATF4—Slow aging—Cell stress resistance—Life span.

Received September 26, 2013; Accepted February 12, 2014

Decision Editor: Rafael de Cabo, PhD

IT is now clear that many of the cellular and intercellular pathways that mediate aging rate and can extend life span in yeast, worms, and flies have parallel effects in mammals (1–4). Signals that modulate function of mammalian target of rapamycin (mTOR) or of insulin-like stimulation of FoxO action are the best characterized, with analyses of sirtuin activities also receiving widespread attention.

Studies in the yeast *Saccharomyces cerevisiae* have shown that mutations that interfere with assembly of the 60S ribosomal subunit, or which limit actions of TOR-dependent ribosomal activation, often extend the life span of yeast replicative clones. Steffen and colleagues (5) have reported that Gcn4 was required for yeast life-span extension induced by deletion of each of 11 tested ribosomal protein genes, and by deletion of yeast TOR1, with a similar trend in experiments that used dietary restriction to extend life span. Gcn4, whose mammalian ortholog is ATF4, is controlled at the translational level through Gcn2 signals. Restriction of glucose or amino acids leads to higher Gcn4 translation, leading to downregulation of expression of many genes, and upregulation of a smaller set of RNAs required for restoration of protein translation (6,7). Steffen's work thus suggests that many forms of yeast life-span extension may be mediated by increases in Gcn4 protein level and require Gcn4-dependent activation of target genes. These yeast experiments motivated us to evaluate the possible involvement of ATF4 translation and induction of ATF4-dependent target genes, in cells and tissues of long-lived mutant mice. There is also some indication that Gcn2 and Gcn4 may contribute to stress resistance

in mice as well. Exposure of mice to diets deficient in amino acids, for example, can increase surgical stress resistance (8), and there is some evidence that deficiency of one of more essential amino acids may mediate the effects of dietary restriction through inactivation of mTORC1 and activation of GCN2 and GCN4/ATF4 pathways (9). The Snell and Ames dwarf mice, homozygous respectively for mutations at the Pit-1 and Prop-1 loci, show extended longevity and retardation of multiple age-dependent changes attributable to diminished pituitary production of growth hormone (GH), thyroid stimulating hormone, and prolactin, with secondary deficits in IGF-1 and thyroxine. These mice are protected against multiple age-associated changes, including alterations in cognition (10), joint pathology (11), immune function (12), cataract risk (13), kidney disease (13), collagen cross-linking (12), and tumor incidence (14), suggesting strongly that these mutants slow the aging process as a whole, and with it thus decelerate multiple effects of aging. Fibroblasts derived from the skin of Snell and Ames dwarf mice are resistant to multiple forms of lethal and metabolic stress (15,16), susceptible to stimuli that induce autophagy (17), and slow to activate extracellular signal-regulated kinase (ERK) (extracellular signal-regulated kinase) phosphorylation after stress, (18) but quick to downregulate mTOR (17), suggesting that they retain a suite of cellular traits presumably induced, in vivo, by hormone-dependent epigenetic switches.

Mutation of pregnancy-associated plasma protein A (PAPP-A), a protease that cleaves some but not all isoforms of IGF-1 binding proteins, also leads to life-span extension

in mice, perhaps because higher levels of PAPP-A-sensitive isoforms of IGF-1 binding proteins reduce effective IGF-1 concentration in some tissues (19). Many age-sensitive forms of pathology are also delayed in the PAPP-A knock-out (KO) mice (20). The properties of skin fibroblasts from PAPP-A mutant mice have not been characterized. Serum levels of GH and IGF-1 are within normal limits in these mutant mice, and it is plausible that the longevity effect is mediated by diminished concentrations of available IGF-1 in one or more tissues in which the level of IGF-1 depends on the balance between serum IGF-1, tissue binding proteins, and PAPP-A protease activity (21).

We report here that fibroblasts from Snell dwarf and PAPP-A KO mice show heightened activity of ATF4, including higher levels of induction of ATF4 target genes, after exposure to multiple forms of stress, and that ATF4 pathways are also elevated in liver of both varieties of long-lived mice.

## MATERIALS AND METHODS

### *Mice*

Snell dwarf and littermate control mice were produced by a cross between (DW/J × C3H/HeJ)-dw/+ heterozygous parents and maintained using husbandry conditions that have been described previously (13). Skin cells for primary fibroblast cultures and liver tissue were derived from 4- to 6-month-old virgin mice. All animal procedures have been approved by the University Committee on Use and Care of Animals at the University of Michigan. The colony is evaluated for specific pathogen status every 3 months, and all such tests have been negative during the period of this study.

### *Cell Culture*

Primary fibroblast cultures were generated using a previously published protocol (16) and studied at the second or third passage. For experiments with tunicamycin, H<sub>2</sub>O<sub>2</sub>, and cadmium, cells were first cultured overnight in 2% bovine serum albumin Dulbecco's modified Eagle medium before addition of the stress agent. For amino acid withdrawal experiments, the cells were first cultured overnight in Minimal Essential Medium (MEM) containing 10% dialyzed fetal bovine serum. Then the culture medium was replaced by Earle's balanced salt solution supplemented with dialyzed fetal bovine serum and vitamin mix for the indicated times.

### *Antibodies and Chemicals*

Anti-ATF4, anti-ATF3, and anti-ASNS were purchased from Santa Cruz (Santa Cruz, CA). Antibodies specific for phospho-GCN2, phospho-EIF2 $\alpha$ , and phospho-PERK were purchased from Cell Signaling (Danvers, MA). Anti-rabbit or mouse IgG horseradish peroxidase-linked secondary

antibody at 1:3,000 to 1:5,000 dilutions was purchased from Invitrogen (Carlsbad, CA). Tunicamycin, hydrogen peroxide, and cadmium were purchased from Sigma (St. Louis, MO).

### *Western Blotting*

To detect protein expression and phosphorylation, cultured primary cells were washed once with cold phosphate buffered saline (PBS) and then lysed in Nonidet P-40 buffer (10 mM Tris-HCl, pH 7.5, 2 mM EDTA, 150 mM NaCl, 1% Nonidet P-40, 50 mM NaF, 1 mM sodium vanadate, 1 mM phenylmethylsulfonyl fluoride, 2  $\mu$ g/ml aprotinin, 2  $\mu$ g/ml leupeptin). The lysates were cleared by centrifugation at 13,000 rpm. The supernatant was used for analyzing protein expression and phosphorylation by western blot.

### *Quantitative Real-Time PCR and Statistical Analysis*

Relative quantities of messenger RNA (mRNA) expression were analyzed using real-time PCR (ABI Prism 7500 Sequence Detection System, Applied Biosystems). The SYBR (Applied Biosystems) green fluorescence dye was used in this study. Paired *t* tests (two-tailed) for one-factor comparisons were used to compare treated cells with control cells. Error bars represent the standard error of the mean. Primer sequences are shown in [Supplementary Table S1](#).

### *Immunofluorescence*

Second passage fibroblast cells derived from tail skin of Snell dwarf and nonmutant littermate control females (4 months of age) were cultured in complete medium on glass at sufficient density to cover 50% of the area. After 24 hours, the culture medium was replaced by MEM containing 10% dialyzed fetal bovine serum. For amino acid deprivation, next day the culture medium was switched to Earle's balanced salt solution supplemented with dialyzed fetal bovine serum and vitamin mix and incubated for 4 hours. The cells were then washed by cold phosphate buffered saline buffer, after which 4% paraformaldehyde was used to fix the cells for 10 minutes. After 5% goat serum blocking, the antibodies ATF4, ATF3, phospho-GCN2, and negative control rabbit IgG were used to incubate overnight. The cells were washed twice with phosphate buffered saline, and the secondary antibody Alexafluor-488-conjugated goat anti-rabbit IgG (H + L chain specific) was used to detect ATF4, ATF3, and p-GCN2. Diamidinophenylindole was used to stain cell nuclei.

### *Liver mRNA and Protein Extraction*

For RNA extraction, about 50–100 mg liver tissue was added to 1 ml Trizol, followed by ultrasonic exposure for 30 seconds. One hundred microliters of chloroform was then added, and the mixture was vortexed for 1 minute and

centrifuged at 13,000rpm for 20 minutes. Supernatants were placed in a new tube and extracted by chloroform a second time. An equal volume of isopropanol was then added to precipitate RNA. The RNA was washed by 75% cold ethanol and dissolved in DEPC-treated water. For protein extraction, about 50–100mg liver sample was added to about 1 ml of NP-40 lysis buffer (10 mM Tris-HCl, pH 7.5, 2 mM EDTA, 150 mM NaCl, 1% Nonidet P-40, 50 mM NaF, 1 mM sodium vanadate, 1 mM phenylmethylsulfonyl fluoride, 2  $\mu$ g/ml aprotinin, 2  $\mu$ g/ml leupeptin). The samples were exposed to ultrasonication for 30 seconds, and then centrifuged at 13,000 rpm for 20 minutes. Supernatants were then removed for analysis after adjustment to equal protein concentration.

#### Treatment of Fibroblasts With Tunicamycin, H<sub>2</sub>O<sub>2</sub>, or Cadmium

Fibroblasts were cultured to near confluence (95%), then incubated in serum-free Dulbecco's modified Eagle medium with 4% bovine serum albumin overnight

(typically 12 hours), and then incubated in serum-free Dulbecco's modified Eagle medium containing either tunicamycin (1  $\mu$ g/ml), H<sub>2</sub>O<sub>2</sub> (50  $\mu$ M), or cadmium (20  $\mu$ M) for the indicated time period, that is, either 1 or 2 hours. Cells were then lysed and processed for immunoblotting as described earlier.

## RESULTS

### Amino Acid Withdrawal Induces Higher ATF4 Levels in Fibroblast Cells Derived From Snell Dwarf Mice

Early passage fibroblasts from skin of adult Snell dwarf mice are hypersensitive to induction of autophagy when cultured in the absence of amino acids (17). To assess the potential involvement of ATF4 in this hypersensitivity, we evaluated the effect of amino acid deprivation on protein levels of ATF4 (Figure 1A and B). We found that amino acid withdrawal did, as hypothesized, lead to higher levels of ATF4 protein in fibroblast cells from Snell dwarf mice. As an independent test of ATF4 induction, we measured

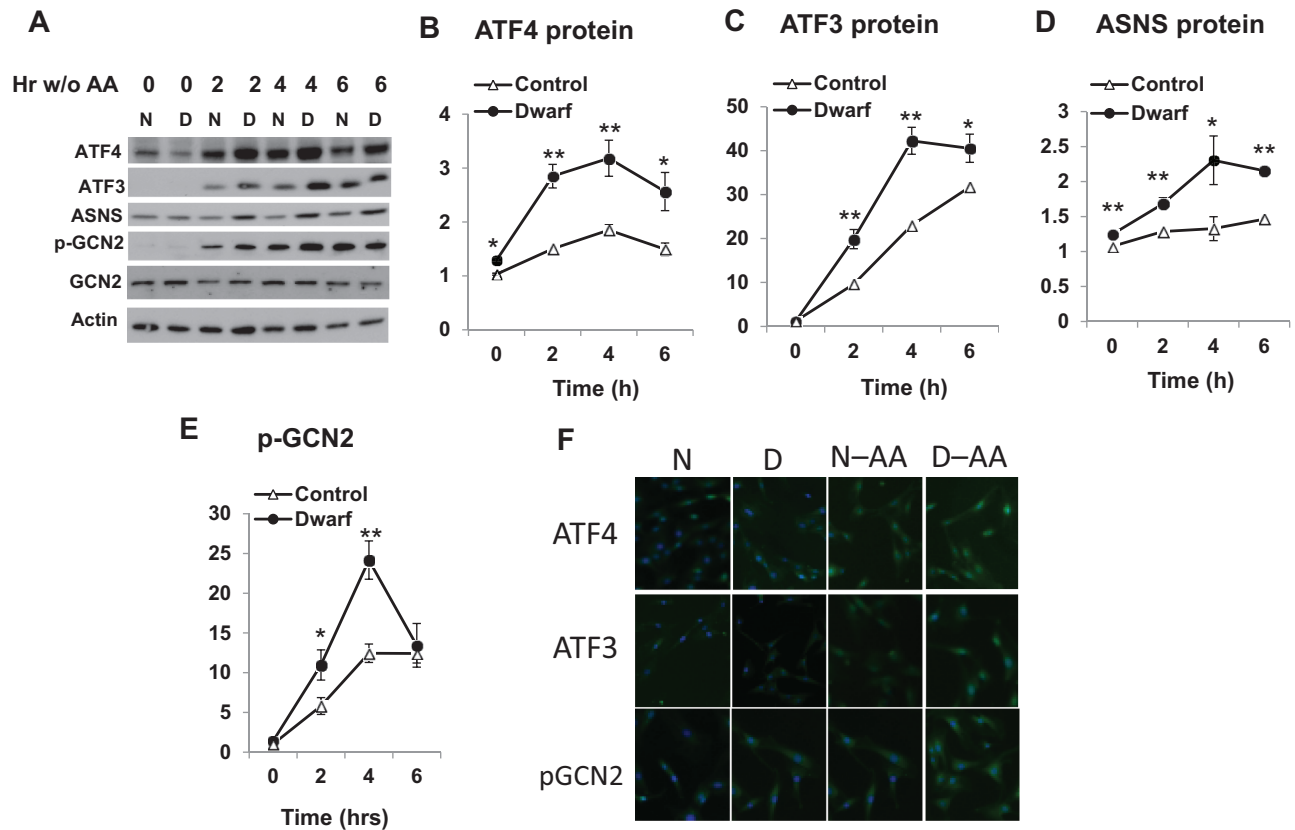


Figure 1. Fibroblasts from Snell dwarf mice show increased levels of ATF4 protein, ATF4 target proteins, and ATF4-inducing signals after amino acid deprivation. Panel (A) shows immunoblot analysis of ATF4, ATF3, ASNS proteins, and phosphorylated forms of GCN2, with actin as a loading control, at 2, 4, or 6 hours after withdrawal of amino acids. N = normal control fibroblasts; D = dwarf fibroblasts. One representative experiment of six performed. Panels (B–E) show quantitation of time course for induction of the indicated protein species in the first 6 hours after amino acid withdrawal by imaging quantification software. Symbols show mean and standard error of the mean (SEM) for  $N = 6$  experiments.  $p$  values: (\*)  $p < .05$ ; (\*\*)  $p < .01$  by Student's  $t$  test. The y-axis represents the relative protein levels of each testing protein normalized with corresponding internal control actin. (F) Immunofluorescence of ATF4, ATF3, and GCN2 phosphorylation after amino acid withdrawal. The first two columns show cells incubated in complete Dulbecco's modified Eagle medium with 10% fetal bovine serum, and the right-hand columns show the effects of 4 hours of incubation in amino acid-deficient medium, Earle's balanced salt solution with 10% dialyzed fetal bovine serum.

the effects of amino acid withdrawal on levels of ATF3 and ASNS, each of which contains a conserved ATF4-binding motif (TGATG) in the promoter region. Each of these proteins was induced more vigorously in fibroblasts from Snell dwarf mice (Figure 1A, C, and D), consistent with the data on ATF4 levels. We also evaluated phosphorylation of the kinase GCN2, an amino acid sensor upstream of ATF4, which is involved in mediating ATF4 induction after amino acid withdrawal. Phosphorylation of GCN2 increased dramatically after amino acid withdrawal, with stronger induction in fibroblast cells from Snell dwarf mice (Figure 1A and E). A third method, immunofluorescence staining, also demonstrated higher expression of ATF4 and ATF3 and higher phosphorylation of GCN2, in fibroblasts of Snell dwarf mice after amino acid withdrawal (Figure 1F).

As a further test of genotype-specific differences in ATF4 function, we evaluated accumulation of ATF4-dependent mRNAs at varying intervals after amino acid withdrawal. Our data (Figure 2) showed enhanced transcription of five such target mRNAs, with slight increases in transcription of ASNS and CAT1 by Snell fibroblasts and larger increases in transcription of ATF3, CHOP, and TRB3 mRNA. We also noted a modest

increase in mRNA levels of ATF4 itself after amino acid withdrawal, with significantly greater effects in Snell-derived cells. In parallel experiments, we also evaluated mRNA levels for SNAT2, xCT, HERP, VEGF, 4E-BP1, C/EBP $\beta$ , Redd1, GADD34, and ATF5 (data not shown), but these did not show significant changes after amino acid withdrawal, in control or dwarf fibroblasts, over the interval chosen for study.

#### Higher Induction of ATF4 in Snell Fibroblasts Exposed to Three Forms of Lethal Stress

Snell dwarf fibroblasts are also unusually resistant to lethal injury induced by cadmium and by H<sub>2</sub>O<sub>2</sub> (15) but unusually susceptible to cell death induced by the endoplasmic reticulum (ER) stress agent tunicamycin (22). We therefore examined expression of ATF4 and its targets in cells exposed to these three agents, using a protocol in which serum is withdrawn for 18 hours prior to stress exposure (to mimic the protocol used for tests of stress resistance) (15,16). A representative immunoblot is shown in Supplementary Figure S1. Each of these three forms of stress led to stronger induction of ATF4 protein

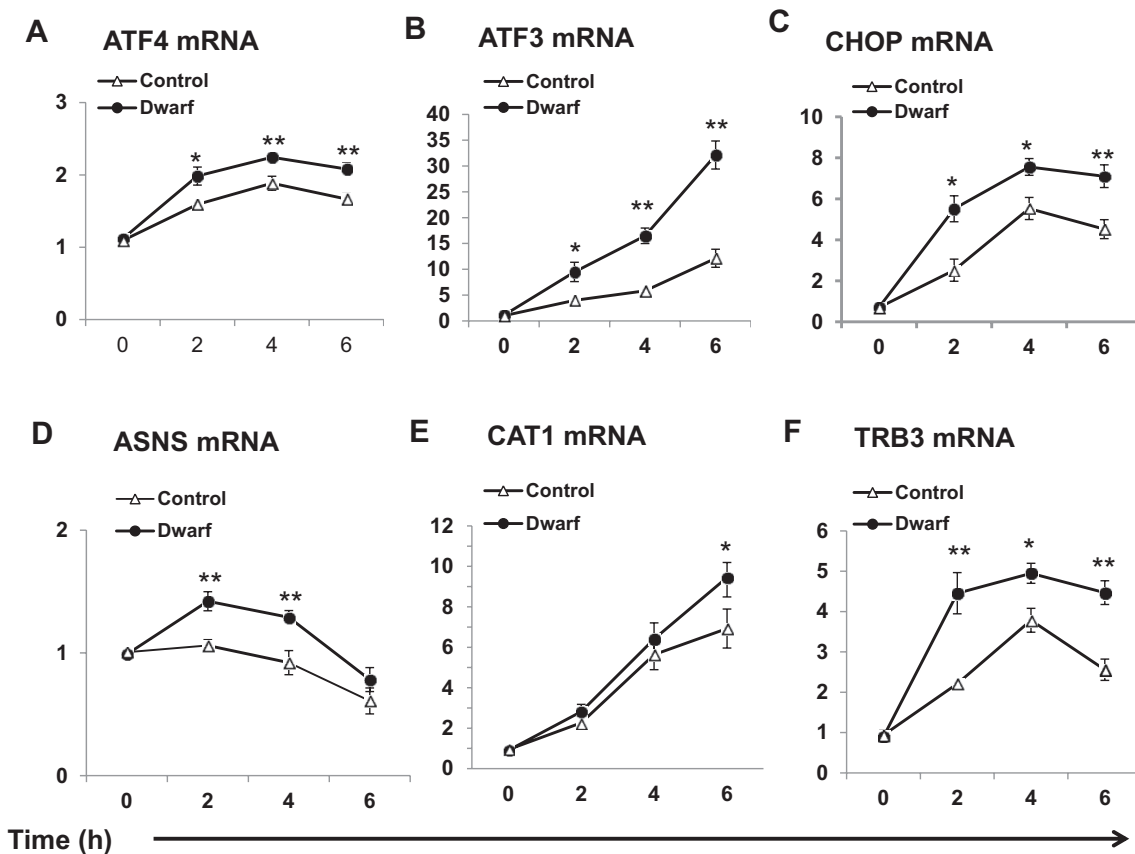


Figure 2. Fibroblasts from Snell dwarf mice show increased induction of several ATF4 target mRNAs after amino acid deprivation. Points show mean and SEM for  $N = 9$  samples of each genotype at each time point. Values have been normalized as a ratio to the level of mRNA in the control cells at  $t = 0$  within each experimental group. Scales vary across panels, as indicated, to reflect differences in the extent of mRNA induction.  $p$  values: (\*)  $p < .05$ ; (\*\*)  $p < .01$  by Student's  $t$  test. The y-axis represents the relative RNA levels of each tested gene normalized with the corresponding internal control glyceraldehyde phosphate dehydrogenase (GAPDH). Panels A-F represent, respectively, mRNA for ATF4, ATF3, CHOP, ASNS, CAT1, and TRB3.

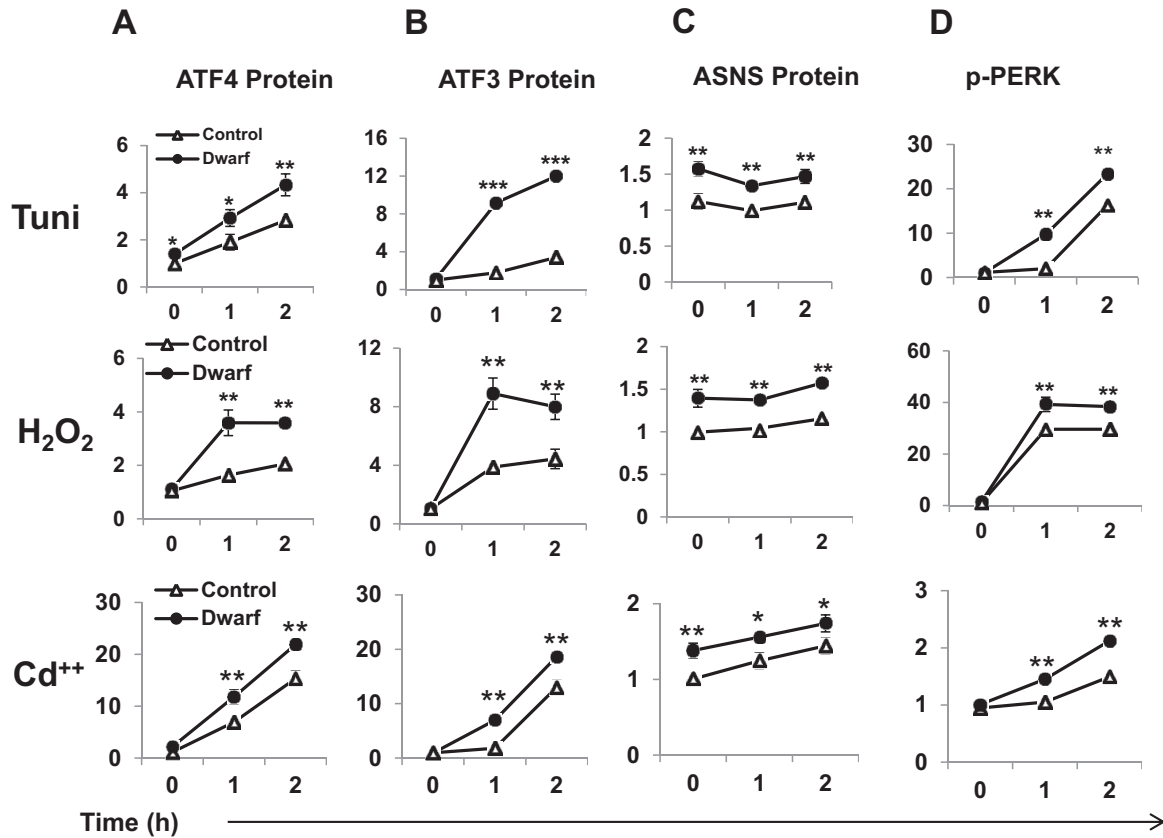


Figure 3. Increased activation of the ATF4 pathway in Snell dwarf fibroblasts after exposure to tunicamycin, H<sub>2</sub>O<sub>2</sub>, or cadmium. Panels (A–D) show quantification of western blot images. Points show mean and SEM for  $N = 6$  samples of each genotype at each time point. Values have been normalized as a ratio to the level of protein in the control cells at  $t = 0$  within each experimental group. Scales vary across panels, as indicated, to reflect differences in the extent of mRNA induction.  $p$  values: (\*)  $p < .05$ ; (\*\*)  $p < .01$ ; (\*\*\*)  $p < .001$  by Student's  $t$  test. The y-axis represents the relative protein levels of each testing protein normalized with corresponding internal control actin.

in dwarf cells than in control cells (Figure 3A). Induction of the ATF4 target ATF3 was also stronger for each stress in the dwarf-derived fibroblasts (Figure 3B). ASNS levels (Figure 3C) were higher in dwarf than in control cells prior to stress, perhaps as a consequence of the overnight incubation in serum-free medium, and remained higher throughout the test period. Phosphorylation of PERK, a kinase important for ATF4 translation after stress exposure, was also more responsive in dwarf than in control cells for each stress. As an independent test of ATF4 activity after stress exposure, we measured mRNA for three target genes, ATF3, CHOP, and ASNS, in stress-exposed fibroblasts (Supplementary Figure S2). Consistent with the data on protein levels in Figure 3, mRNA for ATF3, as well as for CHOP, another ATF4 target, was induced more strongly in Snell dwarf cells in response to each of the three stresses. mRNA for ASNS was elevated in Snell cells prior to stress exposure, and remained so. ATF4 mRNA was also increased by each stress, with higher responses in dwarf cells in the responses triggered by tunicamycin and H<sub>2</sub>O<sub>2</sub>, but not Cd. These results suggest that induction of ATF4 was significantly greater in response to each of these three forms of stress in dwarf-derived fibroblast cells.

#### Transcription of ATF4 and ATF4 Target Genes in Livers of Snell Dwarf Mice

Our fibroblast data showed that expression of ATF4, its upstream signals, and its downstream targets were all elevated in cells from Snell dwarf mice in responses to amino acid withdrawal and multiple forms of stress. To see if similar changes occur in vivo, we evaluated RNA from liver samples of young adult mice, with or without 2 days of fasting. In mice not subjected to fasting, we noted higher mRNA levels for five of these ATF4 target genes, that is, ASNS, ATF3, CHOP, TRB3, and CAT1, in Snell dwarf liver compared with liver of littermate control mice (Figure 4). Fasting produced a significant elevation of four of these five mRNAs ( $p < .01$  except for ASNS), and all five of these target mRNAs were higher in liver of fasted Snell dwarf mice compared with fasted controls. ATF4 mRNA level did not differ between Snell and control liver, but ATF4 protein levels were elevated in Snell liver with or without fasting (Figure 4, panels G, H), consistent with translational control of ATF4 protein. CHOP protein level was elevated in Snell liver, both in nonfasted and in fasted mice, consistent with the implications of the CHOP mRNA analysis. These results show that elevated ATF4 pathways are seen

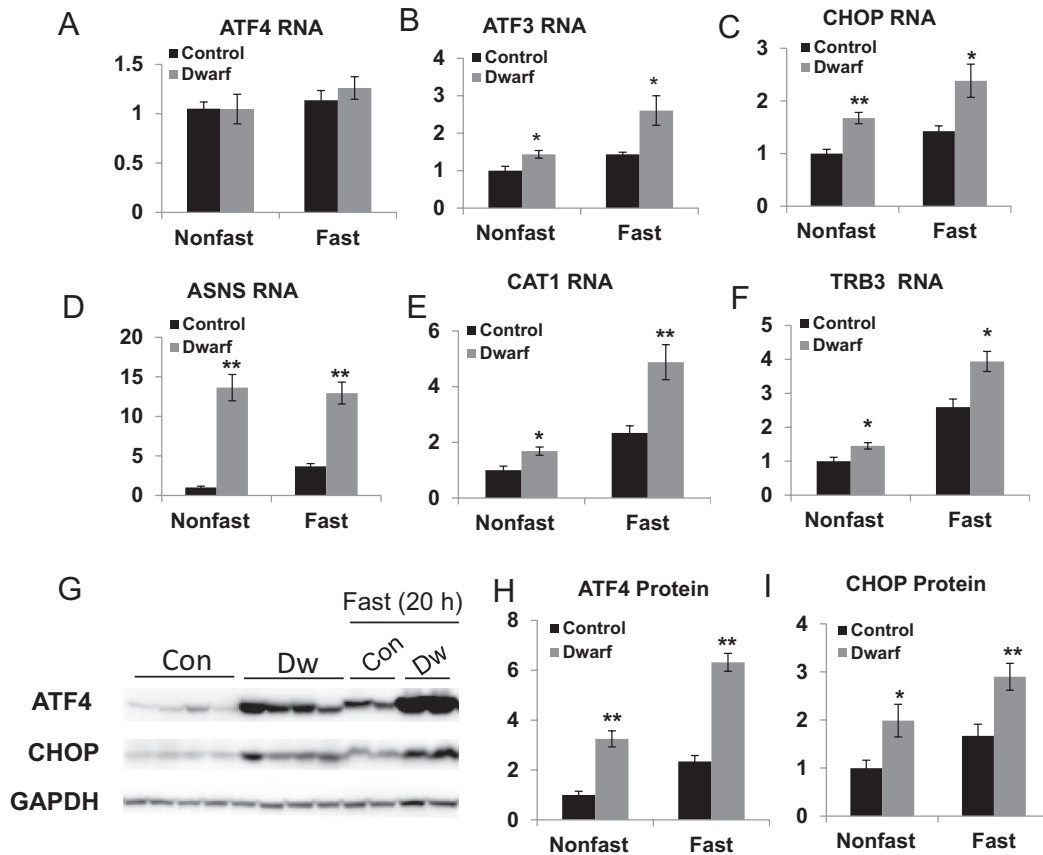


Figure 4. Increased levels of ATF4 target mRNA and proteins in liver of Snell dwarf mice, before and after fasting. Panels (A–F): mRNA levels estimated by quantitative real-time PCR in liver of 4- to 5-month-old female Snell dwarf and littermate control mice. Bars show mean and SEM for  $N = 4$  mice, normalized to the level seen in control mice within each experimental group. (G) Immunoblot analysis of ATF4 and CHOP protein levels in mice not subjected to fasting (columns 1–4) or after 24 hours of fasting (columns 5–8).  $N =$  normal control; DF = Snell dwarf. (H–I): quantification for ATF4 and CHOP protein expression.  $p$  values: (\*)  $p < .05$ ; (\*\*)  $p < .01$  by Student's  $t$  test. The y-axis represents the relative RNA or protein levels of each tested gene normalized with respect to glyceraldehyde phosphate dehydrogenase (GAPDH) or actin as an internal control.

not only in skin-derived fibroblast cell lines but also in liver of adult mice.

#### Augmented ATF4 Signals in Fibroblasts and Liver From PAPP-A KO Mice

We also evaluated fibroblasts from PAPP-A KO mice, another mutant in which alterations in IGF-1 availability lead to extended life span. Figure 5 shows experiments in which fibroblasts from these mice were evaluated after exposure to amino acid-deficient medium. ATF4 protein levels increased to a greater degree in cells from PAPP-A KO mice (Panel A), and ATF3 protein was higher both before and after amino acid withdrawal. Measurement of mRNA for ATF4 target genes (Panel B) showed significantly higher levels of all five mRNA in the PAPP-A KO cells. There were no significant changes in mRNA for ATF4 itself, consistent with the idea that ATF4 protein levels are controlled largely at the translational level in this setting. Induction of ATF4 and ATF3 protein by exposure to cadmium (Panel C) was also higher in the cells from PAPP-A KO mice. These findings are thus

similar to the observations made using fibroblasts from Snell dwarf mice (Figures 1–3).

The results shown in Figure 6 indicate that ATF4 activity is also elevated in liver of PAPP-A KO mice. mRNA for four of the five tested ATF4 target genes (ATF3, CHOP, CAT1, and TRB3 but not ASNS) is elevated in liver of PAPP-A KO mice, both in the fed and fasted conditions. Surprisingly, ASNS mRNA is significantly lower in PAPP-A KO mice in both conditions, suggesting that the PAPP-A mutation may alter ASNS transcription through pathways independent of ATF4 activity. Figure 6 (panels G–I) also shows that both ATF4 and CHOP proteins are at higher levels in fasted and nonfasted PAPP-A KO mice, consistent with the data on mRNA for ATF4 target genes. Thus, the findings in PAPP-A KO liver (except for the unexpected result for ASNS) parallel those seen in PAPP-A KO fibroblasts and in the Snell dwarf system.

#### DISCUSSION

Our data show heightened sensitivity of ATF4 and some of its targets in cultured fibroblasts of two varieties

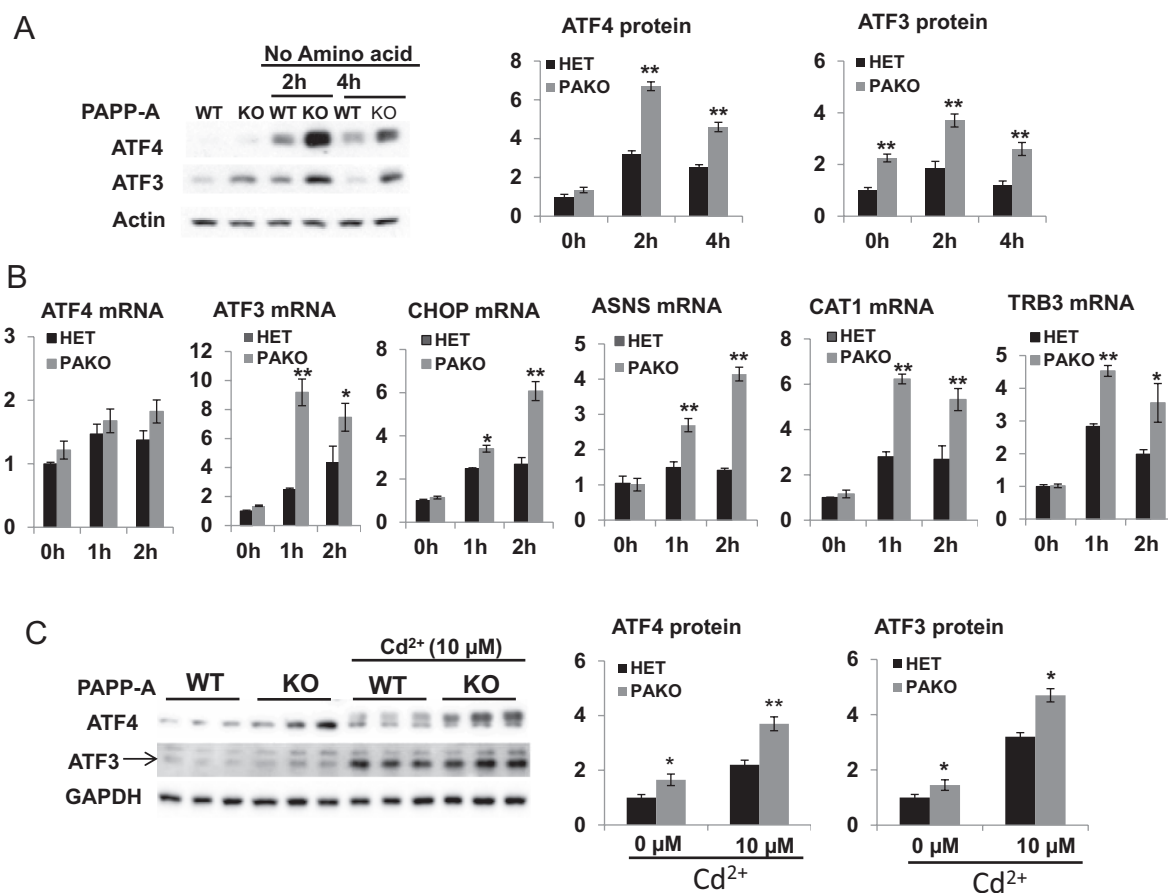


Figure 5. Greater upregulation of the ATF4 pathway in fibroblasts from PAPP-A knockout (KO) mice. Panel A shows immunoblot analysis of ATF4 and ATF3 proteins with actin as a loading control, at 2 and 4 hours after withdrawal of amino acids in fibroblasts derived from control heterozygote littermate (HET) and PAPP-A KO (PAKO) mice. Symbols show mean and SEM for  $N = 6$  experiments. The y-axis represents the relative protein levels of each protein normalized with respect to the corresponding internal control actin. Panel B shows induction of the indicated mRNAs in fibroblasts from PAPP-A KO mice in the first 2 hours after amino acid withdrawal. Points show mean and SEM for  $N = 6$  samples of each genotype at each time point. Values have been normalized as a ratio to the level of mRNA in the control cells at  $t = 0$  within each experimental group. Scales vary across panels, as indicated, to reflect differences in the extent of mRNA induction. Panel C shows cadmium-induced ATF4 and ATF3 expression in PAPP-A KO fibroblast cells and their protein were quantified by immunoblot gel imaging software.  $p$  values: (\*)  $p < .05$ ; (\*\*)  $p < .01$  by Student's  $t$  test. The y-axis represents the relative RNA or protein levels of each tested gene normalized with respect to glyceraldehyde phosphate dehydrogenase (GAPDH) or actin as an internal control.

of long-lived mutant mice, with parallel changes in the liver of both strains. The fibroblast studies show elevated ATF4 action in responses to amino acid withdrawal, the most highly studied stimulus for ATF4 activation, and in responses to chemical stresses, including two that Snell dwarf cells are resistant to (peroxide and Cd), and one, tunicamycin, to which Snell fibroblasts are relatively resistant. The data on liver of intact mice show similar changes in both fed and fasted animals, with the unexplained anomaly of ASNS reduction in liver of the PAPP-A mice (Figure 6E). Pathways upstream of ATF4, specifically Gcn2 in the amino acid withdrawal system and PERK in the stress-response experiments, are also hypersensitive in the Snell fibroblasts. The heightened alertness of ATF4 pathways in cells cultured in vitro represents stable epigenetic controls acquired in the skin and maintained in vitro after explantation, adaptation to culture, and multiple rounds of mitosis. The similar findings in liver suggest that augmented ATF4 responses

may be characteristic of at least some other cell and tissue types in long-lived adult mice.

Conditions that diminish translation, such as amino acid deprivation or ER stress, induce an increase in ATF4 protein levels through an alteration in the translational reading frame of the ATF4 mRNA (reviewed in Kilberg and colleagues) (23). When amino acids are abundant, translation utilizes two open reading frames, uORF1 and uORF2, that are out of frame with the ATF4 coding sequence. In conditions of amino acid scarcity, however, uncharged transfer RNA accumulation leads to activation of GCN2 kinase, which in turn phosphorylates the translation initiation factor eIF2 $\alpha$ . Phosphorylated eIF2 $\alpha$  forms a nonfunctional complex with the guanine nucleotide exchange factor eIF2B to inhibit guanosine triphosphate (GTP)-bound eIF2 complex formation required for uORF1 and uORF2 translation initiation and global translation. Diminished levels of the eIF2-GTP complex lead to ribosomal bypass of uORF2 and

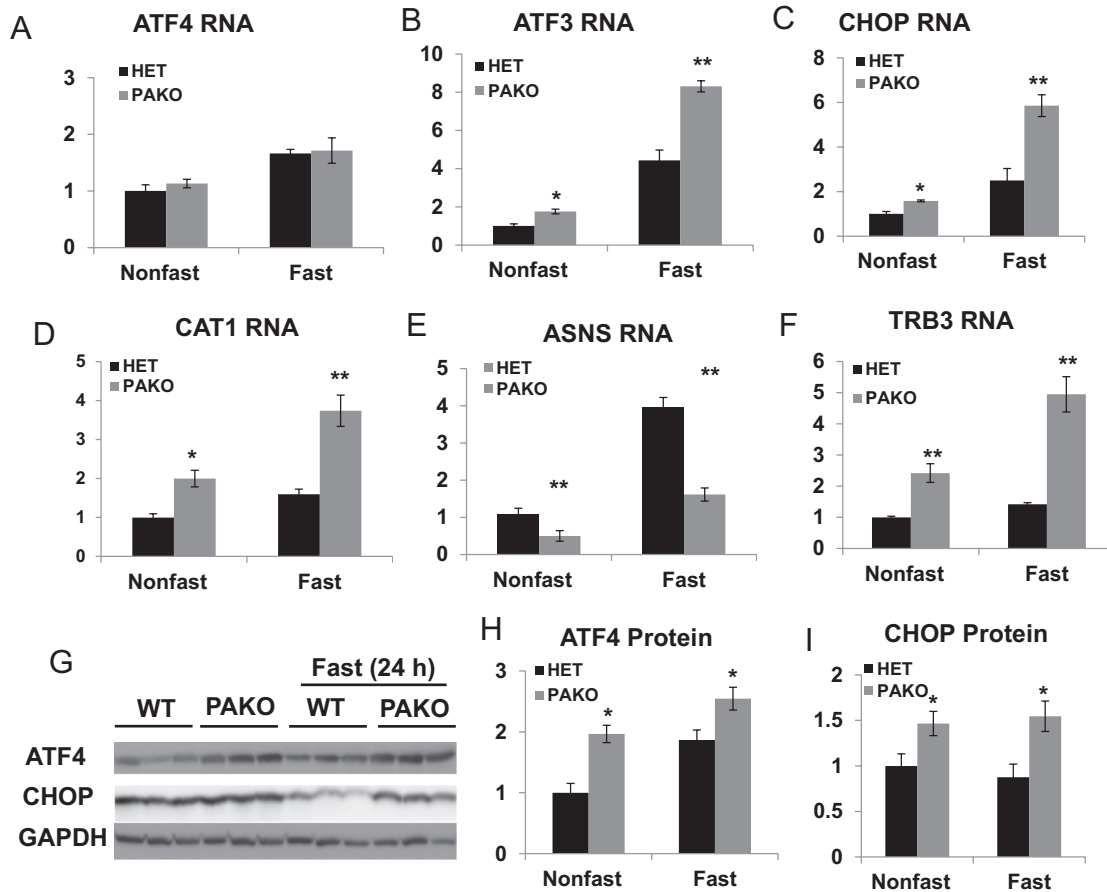


Figure 6. Increased levels of ATF4 targeted gene mRNA and proteins in liver of PAPP-A mice, before and after fasting. (A–F): mRNA levels estimated by quantitative real-time PCR in liver of female PAPP-A KO and littermate control mice, at 4–5 months of age. Bars show mean and SEM for  $N = 3$  mice, normalized to the level seen in control mice within each experimental group. (G) Immunoblot analysis of ATF4 and CHOP protein levels in mice not subjected to fasting (columns 1–6) or after 48 hours of fasting (columns 7–12). (H and I): quantitation of ATF4 and CHOP protein expression from the experiment shown in Panel G. The bar graphic shows mean (and SEM) for  $N = 3$ .  $p$  values: (\*)  $p < .05$ ; (\*\*)  $p < .01$  by Student's  $t$  test. The y-axis represents the relative RNA or protein levels of each tested gene normalized with respect to glyceraldehyde phosphate dehydrogenase (GAPDH) or actin as an internal control.

reinitiation, downstream, at the start of the ATF4 coding region. Thus, ATF4 acts as a switch to upregulate transcription of specific subset of stress-response genes when overall translation is depressed. It will be of interest to evaluate phosphorylation status of eIF2 in various slow-aging mouse populations, including mice treated to the mTOR inhibitor rapamycin (24,25), and those in which life span is extended by partial restriction of methionine (26,27), required for initiation of protein translation.

Control of translation of ATF4 is modulated by at least four protein kinases, GCN2, PERK, PKR, and HRI, each of which is sensitive to different forms of stress. GCN2 is sensitive to amino acid limitation, PERK responds to ER stress, PKR detects double-stranded RNA, and HRI is a sensor for depressed levels of heme (23). All four kinases phosphorylate the same downstream target, eIF2 $\alpha$ . The kinases PERK and eIF2 $\alpha$  are required for ATF4 expression, and therefore PERK $^{-/-}$  cells and kinase dead eIF2 $\alpha^{S51A/S51A}$  knock-in cells, or cells overexpressing an eIF2 $\alpha$  phosphatase (PP1), fail to induce ATF4 expression in response to ER stress (28,29).

However, stress induced by amino acid deprivation and oxidants, which are still able to cause eIF2 $\alpha$  phosphorylation in these cells, does lead to activation of ATF4 (29). GCN2 kinase is required for activation of ATF4: GCN2 $^{-/-}$  cells are impaired for ATF4 expression during amino acid withdrawal (29,30). PKR and HRI are also required for activation of ATF4 in response to specific forms of stress, in that ATF4 expression is impaired in HRI $^{-/-}$  cells exposed to arsenite (31) and in PKR knockdown cells exposed to thapsigargin (32). Studies of ATF4 $^{-/-}$  fibroblast cells showed that ATF4 is responsible for regulation of many target genes, including CHOP and ATF3 (23,29). In addition to translational control of ATF4 levels, some forms of stress regulate ATF4 mRNA at the transcription level (29,33). It will be of interest to see which of these upstream activation pathways might be altered in cells or tissues from mice in which aging has been delayed by mutations, diets, or drug exposure.

We originally speculated that elevation of ATF4 and its targets might play a role in the resistance of Snell fibroblasts to lethal stresses in culture (15), but our data do not



provide unambiguous support for this idea. Snell dwarf fibroblasts are resistant to death induced by H<sub>2</sub>O<sub>2</sub> and cadmium but unusually sensitive to apoptosis induced by the ER stress agents thapsigargin and tunicamycin (22,34). Our new results show elevated ATF4 activity in cells exposed to all three agents tested, that is, H<sub>2</sub>O<sub>2</sub>, cadmium, and tunicamycin, and suggest that the relation between apoptotic pathways and ATF4 activation is not a simple one but may depend on costimulation of cellular pathways that differ among various forms of stress. Additional studies will be needed to clarify these relationships, including explicit studies of upstream controls and evaluation of cells in which ATF4 levels have been increased or decreased prior to stress exposure.

Our data show that fibroblasts and liver from PAPP-A KO mice resemble those from Snell dwarf mice with respect to ATF4 activity. PAPP-A is a protease that cleaves some, but not all, members of the family of IGF-1 binding proteins (21). The mechanism by which PAPP-A deletion leads to life-span extension (35) is not yet clear but seems likely to reflect diminished effective IGF-1 concentration in one or more tissues critical to aging and life-span determination. PAPP-A KO mice have levels of serum GH and IGF-1 that are similar to those of littermate controls with normal life span (35). The evidence that alterations of the ATF4 pathway seen in fibroblasts (Figure 5) and liver of PAPP-A KO mice (Figure 6) are similar to those seen in Snell dwarf mice suggests that altered IGF-1 signals may lie at the root of the changes in cell responses, though alternate explanations can also be constructed. Studies of ATF4 signals in other tissues of these and other varieties of slow-aging mice are likely to help clarify these ideas.

Work in yeast has shown that mTOR may be involved in modulating ATF4 translation. Thus, it seems plausible that lower tissue levels of IGF-1, in both Snell and PAPP-A KO mice, might alter ATF4 pathways through mTOR-dependent processes. Studies in which GH was injected into Ames dwarf mice for several weeks starting just prior to weaning, however, show that early-life exposure to GH and/or IGF-1 can lead to permanent changes in cell properties, including changes in stress responses of skin-derived fibroblasts, which persist even after GH/IGF-1 levels return to the normal low levels characteristic of Ames (and Snell) dwarf mice (36). We would thus predict that ATF4 function in the cultured fibroblasts may be a trait that does not depend on GH/IGF-1 signals per se. We have noted previously differences in mTOR responses to amino acid withdrawal in fibroblasts from Snell dwarf and growth hormone receptor KO mice (17), and so we think the idea that altered mTOR signals might contribute to differences in ATF4 responses deserves careful study in our next set of in vitro experiments.

Our data certainly do not prove that altered ATF4 responses, in liver or any other tissue, must necessarily contribute to the longevity and disease resistance of Snell dwarf and PAPP-A KO mice, but the requirement for the ATF4

homolog Gcn4 for extended longevity of yeast cells in several situations (5) makes it seem plausible that ATF4 may play a role in regulation of aging in mice. There is ample evidence that both aging rate and many aging-related diseases can be affected by stress-response and repair pathways (37). Aging leads to a decline in levels of ATF4 and in expression of ATF4-sensitive genes, as well as in pathways that modulate ATF4 activity such as eIF2 $\alpha$ , PERK, and PKR (38), suggesting that ATF4 and the ATF4 stress responsive pathway may help to regulate aging and age-dependent diseases.

Studies of longevity in lower organisms can provide valuable clues to mechanisms that control aging rate in mammals, but it can be difficult to sort authentic clues, reflecting evolutionary conservation or parallel evolution, from red herrings related to species-specific idiosyncrasies. Some of the genes that influence replicative (clonal) senescence in budding yeast (*S. cerevisiae*) have been shown to modulate longevity in worms (39) and flies (40,41), and parallel cellular systems are also implicated in control of mouse aging rate (42,43). Other pathways that control yeast life span, such as extrachromosomal DNA circles, appear to reflect species-specific or "private" pathways (44). Our results in liver of Snell and PAPP-A mice show that the connection of ATF4 to life span may have deep evolutionary roots, and the fibroblast system should provide opportunities to evaluate the molecular determinants and consequences of ATF4 hypersensitivity. Further attention to the signals that control ATF4, and to its downstream targets, in invertebrate models is likely to provide a fast and economical way to study the implications of our mouse study and help to motivate work on ATF4 in human age-related diseases. Pharmacological manipulation of ATF4 and its targets could also provide a new approach toward development of medicines to slow aging and postpone multiple age-dependent diseases.

#### SUPPLEMENTARY MATERIAL

Supplementary material can be found at: <http://biomedgerontology.oxfordjournals.org/>

#### FUNDING

This work was supported by National Institutes of Health grants P01-AG031736 and P30-AG013283.

#### ACKNOWLEDGMENTS

We thank Dr. Cheryl Conover for her gift of breeding stock for the PAPP-A knockout mice, and Lisa Burmeister, Sabrina Van Roekel, and Lynn Winkleman for technical assistance.

#### REFERENCES

1. Tatar M, Bartke A, Antebi A. The endocrine regulation of aging by insulin-like signals. *Science*. 2003;299:1346–1351.
2. Kenyon CJ. The genetics of ageing. *Nature*. 2010;464:504–512.
3. Longo VD, Finch CE. Evolutionary medicine: from dwarf model systems to healthy centenarians? *Science*. 2003;299:1342–1346.
4. Bartke A. Single-gene mutations and healthy ageing in mammals. *Philos Trans R Soc Lond B Biol Sci*. 2011;366:28–34.

5. Steffen KK, MacKay VL, Kerr EO, et al. Yeast life span extension by depletion of 60s ribosomal subunits is mediated by Gcn4. *Cell*. 2008;133:292–302.
6. Yang R, Wek SA, Wek RC. Glucose limitation induces GCN4 translation by activation of Gcn2 protein kinase. *Mol Cell Biol*. 2000;20:2706–2717.
7. Hinnebusch AG. Translational regulation of GCN4 and the general amino acid control of yeast. *Annu Rev Microbiol*. 2005;59:407–450.
8. Peng W, Robertson L, Gallinetti J, et al. Surgical stress resistance induced by single amino acid deprivation requires Gcn2 in mice. *Sci Transl Med*. 2012;4:118ra11. doi:10.1126/scitranslmed.3002629
9. Gallinetti J, Harputlugil E, Mitchell JR. Amino acid sensing in dietary-restriction-mediated longevity: roles of signal-transducing kinases GCN2 and TOR. *Biochem J*. 2013;449:1–10.
10. Kinney BA, Meliska CJ, Steger RW, Bartke A. Evidence that Ames dwarf mice age differently from their normal siblings in behavioral and learning and memory parameters. *Horm Behav*. 2001;39:277–284.
11. Silberberg R. Articular aging and osteoarthritis in dwarf mice. *Pathol Microbiol*. 1972;38:417–430.
12. Flurkey K, Papaconstantinou J, Miller RA, Harrison DE. Lifespan extension and delayed immune and collagen aging in mutant mice with defects in growth hormone production. *Proc Natl Acad Sci USA*. 2001;98:6736–6741.
13. Vergara M, Smith-Wheelock M, Harper JM, Sigler R, Miller RA. Hormone-treated snell dwarf mice regain fertility but remain long lived and disease resistant. *J Gerontol A Biol Sci Med Sci*. 2004;59:1244–1250.
14. Ikeno Y, Bronson RT, Hubbard GB, Lee S, Bartke A. Delayed occurrence of fatal neoplastic diseases in ames dwarf mice: correlation to extended longevity. *J Gerontol A Biol Sci Med Sci*. 2003;58:291–296.
15. Murakami S, Salmon A, Miller RA. Multiplex stress resistance in cells from long-lived dwarf mice. *FASEB J*. 2003;17:1565–1566.
16. Salmon AB, Murakami S, Bartke A, Kopchick J, Yasumura K, Miller RA. Fibroblast cell lines from young adult mice of long-lived mutant strains are resistant to multiple forms of stress. *Am J Physiol Endocrinol Metab*. 2005;289:E23–E29.
17. Wang M, Miller RA. Fibroblasts from long-lived mutant mice exhibit increased autophagy and lower TOR activity after nutrient deprivation or oxidative stress. *Aging Cell*. 2012;11:668–674.
18. Sun LY, Steinbaugh MJ, Masternak MM, Bartke A, Miller RA. Fibroblasts from long-lived mutant mice show diminished ERK1/2 phosphorylation but exaggerated induction of immediate early genes. *Free Radic Biol Med*. 2009;47:1753–1761.
19. Boldt HB, Conover CA. Pregnancy-associated plasma protein-A (PAPP-A): a local regulator of IGF bioavailability through cleavage of IGFBPs. *Growth Horm IGF Res*. 2007;17:10–18.
20. Conover CA, Bale LK, Mader JR, Mason MA, Keenan KP, Marler RJ. Longevity and age-related pathology of mice deficient in pregnancy-associated plasma protein-A. *J Gerontol A Biol Sci Med Sci*. 2010;65:590–599.
21. Conover CA. PAPP-A: a new anti-aging target? *Aging Cell*. 2010;9:942–946.
22. Sadighi Akha AA, Harper JM, Salmon AB, et al. Heightened induction of proapoptotic signals in response to endoplasmic reticulum stress in primary fibroblasts from a mouse model of longevity. *J Biol Chem*. 2011;286:30344–30351.
23. Kilberg MS, Shan J, Su N. ATF4-dependent transcription mediates signaling of amino acid limitation. *Trends Endocrinol Metab*. 2009;20:436–443.
24. Harrison DE, Strong R, Sharp ZD, et al. Rapamycin fed late in life extends lifespan in genetically heterogeneous mice. *Nature*. 2009;460:392–395.
25. Miller RA, Harrison DE, Astle CM, et al. Rapamycin, but not resveratrol or simvastatin, extends life span of genetically heterogeneous mice. *J Gerontol A Biol Sci Med Sci*. 2011;66:191–201.
26. Maynard SP, Miller RA. Fibroblasts from long-lived Snell dwarf mice are resistant to oxygen-induced in vitro growth arrest. *Aging Cell*. 2006;5:89–96.
27. Sun L, Sadighi Akha AA, Miller RA, Harper JM. Life-span extension in mice by preweaning food restriction and by methionine restriction in middle age. *J Gerontol A Biol Sci Med Sci*. 2009;64:711–722.
28. Harding HP, Zhang Y, Bertolotti A, Zeng H, Ron D. Perk is essential for translational regulation and cell survival during the unfolded protein response. *Mol Cell*. 2000;5:897–904.
29. Harding HP, Zhang Y, Zeng H, et al. An integrated stress response regulates amino acid metabolism and resistance to oxidative stress. *Mol Cell*. 2003;11:619–633.
30. Hamanaka RB, Bennett BS, Cullinan SB, Diehl JA. PERK and GCN2 contribute to eIF2alpha phosphorylation and cell cycle arrest after activation of the unfolded protein response pathway. *Mol Biol Cell*. 2005;16:5493–5501.
31. Suragani RN, Zachariah RS, Velazquez JG, et al. Heme-regulated eIF2α kinase activated Atf4 signaling pathway in oxidative stress and erythropoiesis. *Blood*. 2012;119:5276–5284.
32. Lee ES, Yoon CH, Kim YS, Bae YS. The double-strand RNA-dependent protein kinase PKR plays a significant role in a sustained ER stress-induced apoptosis. *FEBS Lett*. 2007;581:4325–4332.
33. Dey S, Baird TD, Zhou D, Palam LR, Spandau DF, Wek RC. Both transcriptional regulation and translational control of ATF4 are central to the integrated stress response. *J Biol Chem*. 2010;285:33165–33174.
34. Salmon AB, Sadighi Akha AA, Buffenstein R, Miller RA. Fibroblasts from naked mole-rats are resistant to multiple forms of cell injury, but sensitive to peroxide, ultraviolet light, and endoplasmic reticulum stress. *J Gerontol A Biol Sci Med Sci*. 2008;63:232–241.
35. Conover CA, Bale LK. Loss of pregnancy-associated plasma protein A extends lifespan in mice. *Aging Cell*. 2007;6:727–729.
36. Panici JA, Harper JM, Miller RA, Bartke A, Spong A, Masternak MM. Early life growth hormone treatment shortens longevity and decreases cellular stress resistance in long-lived mutant mice. *FASEB J*. 2010;24:5073–5079.
37. Haigis MC, Yankner BA. The aging stress response. *Mol Cell*. 2010;40:333–344.
38. Hussain SG, Ramaiah KV. Reduced eIF2alpha phosphorylation and increased proapoptotic proteins in aging. *Biochem Biophys Res Commun*. 2007;355:365–370.
39. Smith ED, Kennedy BK, Kaerberlein M. Genome-wide identification of conserved longevity genes in yeast and worms. *Mech Ageing Dev*. 2007;128:106–111.
40. Clancy DJ, Gems D, Harshman LG, et al. Extension of life-span by loss of CHICO, a Drosophila insulin receptor substrate protein. *Science*. 2001;292:104–106.
41. Tatar M, Kopelman A, Epstein D, Tu MP, Yin CM, Garofalo RS. A mutant Drosophila insulin receptor homolog that extends life-span and impairs neuroendocrine function. *Science*. 2001;292:107–110.
42. Kim SK. Common aging pathways in worms, flies, mice and humans. *J Exp Biol*. 2007;210(Pt 9):1607–1612.
43. Bartke A, Coschigano K, Kopchick J, et al. Genes that prolong life: relationships of growth hormone and growth to aging and life span. *J Gerontol A Biol Sci Med Sci*. 2001;56:B340–B349.
44. Sinclair DA, Guarente L. Extrachromosomal rDNA circles—a cause of aging in yeast. *Cell*. 1997;91:1033–1042.